Elastic sheet method for identifying atoms in molecules

Blas P. Uberuaga, Enrique R. Batista, and Hannes Jónsson[a)]
Department of Physics, Box 351560, University of Washington, Seattle, Washington 98195-1560, and Department of Chemistry, Box 351700, University of Washington, Seattle, Washington 98195-1700

(Received 11 January 1999; accepted 17 September 1999)

We have developed a new method for finding and representing dividing surfaces which can, for example, be used to identify ''atoms'' in molecules or condensed phases based on Bader's definition. Given the total electron density of the system, the dividing surface is taken to be the zero-flux surface, i.e., the surface on which the normal component of the gradient vanishes. Our method for finding this surface involves creating an ''elastic sheet'' represented by a swarm of fictitious particles which interact with each other so as to give a nearly uniform distribution of points on the sheet. Two kinds of forces act on the particles: (1) the component of the gradient of the density normal to the elastic sheet, and (2) an interparticle force which only acts in the local tangent plane of the sheet. Starting with a spherical surface and applying an optimization algorithm that minimizes the forces leads to convergence of the particles to the zero-flux surface. The elastic sheet tends to round off regions where the zero-flux surface has sharp cusps or points, but this appears not to be a serious problem in cases we have studied. The elastic sheet method is robust and can converge in situations where currently used methods fail. We demonstrate the method with a study of water clusters and a Si interstitial in a Si crystal.
[S0021-9606(99)70147-9]

I. INTRODUCTION

Studies of molecules and condensed phases often lead to discussions of charges and multipole moments of individual fragments such as atoms or molecules. Given the continuous electronic density of the system, the question becomes how to identify an atom in a molecule, or a molecule in a cluster or a liquid configuration, for example. Many different partitioning schemes have been proposed. When a calculation of the electronic wave function of a system is carried out in terms of atomic basis functions, it is tempting to assign the electronic density associated with a given basis function to the atom at the site.[1] But, it is important to realize that atomic basis sets are overcomplete and such a decomposition is not unique. In principle, a calculation could be done where all the basis functions are located on one of the atoms in the system, which would then lead to an assignment of all the electrons in the system to that one atom.

One compelling way of approaching this problem in a less arbitrary fashion is the decomposition of the charge density proposed by Bader.[2] Here each point in space is assigned to one of the subsystems (e.g., atoms). The dividing surface is chosen to be a zero-flux surface as defined by

$$\nabla \rho \cdot \mathbf{n} = 0, \tag{1}$$

where $\mathbf{n}$ is the surface normal. That is, at every point on a zero-flux surface the gradient of the charge density has no component normal to the surface. Bader has given theoretical arguments as to why this is a good choice for a dividing surface. By using the zero-flux surface, various surface integral terms go to zero when quantum mechanical expectation values for the subsystem are calculated. It can be shown, in particular, that each subsystem defined in this way satisfies a virial theorem.[2]

Finding the zero-flux surfaces of the charge density, however, is not trivial. Methods currently employed can, in fact, fail for certain charge density topologies. The method of Stefanov and Cioslowski,[3] used in the Gaussian code, is one example. This method involves fitting the surface with variational trial functions in prolate spheroidal coordinates. It can fail when the zero-flux surface has certain topological features, such as very strong curvature.[4] During a study of molecular multipole moments of water clusters, we found that the method failed on the hexamer. For this reason, we decided to develop an alternative method for finding zero-flux surfaces.

II. OVERVIEW OF THE ELASTIC SHEET METHOD

In finding a zero-flux surface, we want to minimize the gradient of some scalar field—in this case, the charge density—normal to a closed surface. Our method involves defining a set of fictitious particles which essentially give a discrete representation of the surface. Initially, the particles are distributed randomly on some closed surface, such as a sphere, but are then relaxed according to the force acting on them, and in the end they are located on the zero-flux surface. The force on these particles has two components. The first is the ''real'' force, the gradient of the charge density. The second component is an interaction between the particles which keeps the particles distributed evenly on the surface of the sheet. This force is referred to as the ''distributing'' force. The component of the real force tangent to the sheet surface is zeroed, as is the component of the distribut-

a)Electronic mail: hannes@u.washington.edu

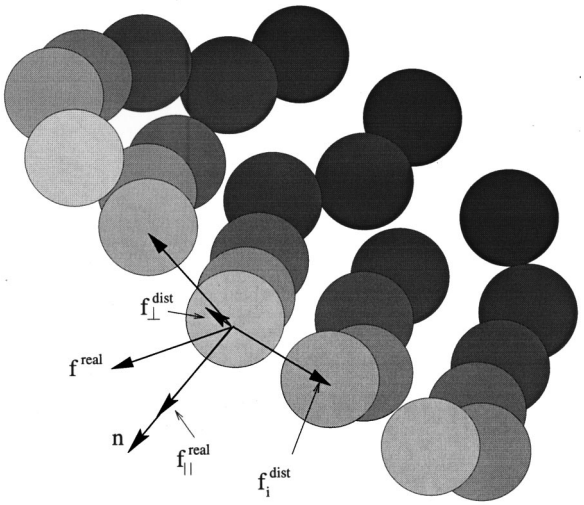

FIG. 1. Forces acting on a particle in the elastic sheet. The particles move in response to the normal component of the real force (gradient of the electronic charge density) and the component of the distributing forces in the local tangent plane. The first acts to move the particles to the zero-flux surface while the second acts to keep the particle distribution nearly uniform.

ing force normal to the sheet. This force projection ensures that the distributing force does not interfere with the relaxation of the particles to the zero-flux surface and guarantees that the real force does not affect the distribution of particles within the surface. As a result, the final shape of the sheet will be determined solely by the charge density, while the distributing force will insure that the density of particles on the surface remains more or less uniform. Figure 1 illustrates the projection of the forces.

In regions where the gradient of the electronic density is small, one can encounter a problem which we refer to as ''kinkiness'': the sheet will form small ripples and particles can ''evaporate'' away from the sheet. To counteract this, an additional restoring force is introduced, the nature of which will be discussed below.

The elastic sheet (ES) method can be viewed as an extension of the nudged elastic band (NEB) method for finding minimum energy paths.[5] In the NEB method, a minimum energy path is represented by a discrete set of fictitious particles whose position is optimized by minimizing the perpendicular component of the gradient of the potential under consideration and the parallel component of a spring force between the particles. The spring force causes the particle to be equidistant along the path (when equal spring constants are used). Because only the parallel component of the spring force is kept, the particles relax to the minimum energy path; the spring force only affects the distribution of particles along the path.

III. DETAILS OF THE ELASTIC SHEET METHOD

The evolution of the ES is governed by two forces: the real force and the distributing force. The real force is just the gradient of the logarithm of the charge density

$$\mathbf{f}_{\parallel}^{\text{real}} = -\frac{1}{\rho}\nabla \cdot \mathbf{nn}. \tag{2}$$

The charge density decays exponentially and the real force would as well. To accelerate convergence in regions where the density is changing slowly, we work with the logarithm of ρ. For finite systems, such as clusters, where the charge density decays to zero, the real force is set to zero at some predefined density contour, which then defines a practical approximation to the zero-flux surface in that direction.

The distributing force acts between the particles that make up the sheet and its purpose is to keep the density of particles on the surface uniform. After testing various types of interactions, we have chosen to use a generalized Lennard-Jones interaction, where the potential energy between particles i and j is given by

$$V_{ij}^{\text{dist}} = \begin{cases} 4\epsilon\left(\dfrac{\sigma^m}{r_{ij}^m} - \dfrac{\sigma^n}{r_{ij}^n}\right) + 4r_{ij}\epsilon\left(m\dfrac{\sigma^m}{r_{\text{cut}}^{m+1}} - n\dfrac{\sigma^n}{r_{\text{cut}}^{n+1}}\right) + K & \\ & r_{ij} < r_{\text{cut}} \\ 0 & r_{ij} > r_{\text{cut}} \end{cases}. \tag{3}$$

Here, ϵ is a parameter defining the strength of the interaction, r_{ij} is the distance between i and j, σ is a parameter that characterizes the current spatial distribution of particles, r_{cut} is a cutoff radius, which we define to be some multiple of σ, and K is a constant that makes V go to zero at r_{cut}. m and n are parameters that define the shape of the interaction. We use $\epsilon = 0.5$, $m = 7$, $n = 6$, and $r_{\text{cut}} = 2.5\sigma$.

This results in the following force between i and j:

$$\mathbf{f}_{ij}^{\text{dist}} = \left[4\epsilon\left(m\frac{\sigma^m}{r_{ij}^{m+1}} - n\frac{\sigma^n}{r_{ij}^{n+1}}\right) - 4\epsilon\left(m\frac{\sigma^m}{r_{\text{cut}}^{m+1}} - n\frac{\sigma^n}{r_{\text{cut}}^{n+1}}\right)\right]\hat{\mathbf{r}}_{ij}, \tag{4}$$

which, because of the second term, goes smoothly to zero at r_{cut}. Here, $\mathbf{f}_{ij}^{\text{dist}}$ is the distributing force on i due to neighbor j and $\hat{\mathbf{r}}_{ij}$ is the unit vector connecting the two particles, $\mathbf{f}_{ij}^{\text{dist}} = 0$ if $r_{ij} > r_{\text{cut}}$.

Because the shape of the elastic sheet changes with time, expanding and contracting, the average distance between particles will also change. To keep the magnitude of the distributing force comparable to that of the real force, as well as to keep the distributing force from either diverging or becoming negligibly small, σ is tuned to the current distribution of the particles on the sheet. We define σ to be the average distance to the closest six neighbors of each particle divided by a parameter α which determines on which side of the potential well minimum the nearest neighbors lie. We use $\alpha = 1$ so the nearest neighbor particles lie on the repulsive side of the well. We have found that it is necessary to update σ every time step. Otherwise, the change in the potential between i and j is too sudden, and there can be problems with stability.

As stated above, the various forces need to be projected onto the surface normal. It is very important to have a good estimate of the normal at each particle at each step during the optimization. We have found that a good estimation of the surface normal is, for example, important for keeping the particles from ''evaporating'' from the elastic sheet. We cal-

culate the normal by first finding three neighbors, *j*, *k*, and *l*, that satisfy the following criteria: Neighbors *j* and *k* are chosen from the six closest neighbors, denoted by $\{n\}$, so that the angle between r_{ij} and r_{ik} is closest to $2\pi/3$. *l* is the neighbor remaining among $\{n\}$ such that the angle between r_{il} and both r_{ij} and r_{ik} is closest to $2\pi/3$. More precisely: Defining

$$f_{jk}=\left|\frac{\mathbf{r}_{ij}\cdot\mathbf{r}_{ik}}{|\mathbf{r}_{ij}|\,|\mathbf{r}_{ik}|}+\frac{1}{2}\right|, \tag{5}$$

The particles *j*, *k*, and *l* are chosen from $\{n\}$ such that

$$\begin{aligned} &j \text{ and } k \text{ minimize } f_{jk} \\ &l \text{ minimizes } f_{jl} \text{ and } f_{kl}. \end{aligned} \tag{6}$$

The normal is then defined as

$$\mathbf{n}=\frac{\mathbf{r}_{jk}\times\mathbf{r}_{jl}}{|\mathbf{r}_{jk}\times\mathbf{r}_{jl}|}. \tag{7}$$

This normal is then used for the force projections at each particle.

At times, one finds particles that drift away slightly from the rest of the sheet. This then leads to inaccuracies in calculating the normals, and these inaccuracies can propagate to nearby particles. To fix this problem, ''smoothing'' is introduced. Smoothing involves adding a force along the direction of the normal to pull the drifting particle back toward the surface of the sheet. The smoothing force is a function of the projected distance of a particle along the normal from the six nearest neighbors, $\{n\}$,

$$z=\frac{1}{6}\sum_{\{n\}}(\mathbf{r}_j-\mathbf{r}_i)\cdot\mathbf{n}. \tag{8}$$

This definition assumes a convention where all normal vectors point away from the inside. This is enforced by keeping track of the direction of the normal at each iteration, all the way from the initial sphere. This works since the direction of the normal cannot flip in one iteration (unless the iteration step size is much too large).

The smoothing adjusts the force in the normal direction so as to pull particles along their normal toward the average plane defined by $\{n\}$.

The form of the smoothing function is

$$s=\begin{cases} -\frac{1}{2}\left(1-\cos\left(\frac{\pi|z|}{\beta\sigma}\right)\right) & \text{if } 0<|z|<\beta\sigma \\ -1 & \text{if } |z|>\beta\sigma \end{cases}. \tag{9}$$

s is negative if $0<z<\beta\sigma$. Here, β is a parameter that determines the range of the smoothing function. The smaller the choice for β, the faster the smoothing force is turned on. We have been using values between 0.5 and 1.0 for β. σ is the parameter used in the definition of the distributing force.

The form of the smoothing force is

$$\mathbf{f}_i^{\text{switch}}=s\times k\times z\mathbf{n}, \tag{10}$$

where *k* is a parameter that determines the strength of the smoothing force. We have used a value between 50 and 100 Å^{-2}.

The final force on particle *i* is then, after zeroing the appropriate components and adding the smoothing force,

$$\mathbf{f}=\mathbf{f}_{\parallel i}^{\text{real}}+\mathbf{f}_{\perp i}^{\text{dist}}+\mathbf{f}_i^{\text{switch}}, \tag{11}$$

where

$$\mathbf{f}_{\parallel}^{\text{real}}=-\frac{1}{\rho}\nabla\rho\cdot\mathbf{nn}, \tag{12}$$

$$\mathbf{f}_{\parallel}^{\text{dist}}=-\nabla V^{\text{dist}}\cdot\mathbf{nn}, \tag{13}$$

$$\mathbf{f}_{\perp}^{\text{dist}}=-\nabla V^{\text{dist}}-\mathbf{f}_{\parallel}^{\text{dist}}, \tag{14}$$

$$\mathbf{f}^{\text{switch}}=s\times k\times z\mathbf{n}. \tag{15}$$

The sheet is minimized with these forces using a minimization method based on the velocity Verlet algorithm[6] where the component of the velocity perpendicular to the force is zeroed at each iteration and the entire velocity vector is zeroed if $\mathbf{v}\cdot\mathbf{f}<0$. When the forces on the particles have been minimized, their position gives a discrete representation of the zero-flux surface.

IV. INTEGRATING THE SUBSPACE DEFINED BY THE ZERO-FLUX SURFACE

Once the zero-flux surface is known, one would like to calculate various properties of the subspace so defined. Most importantly, one would like to know the total charge contained within the surface. Another property that may be of interest is dipole moment, or higher multipole moments. It is, therefore, important to be able to tell which points on the charge density grid lie within the region enclosed by the dividing surface.

This is accomplished by starting with some reference point, $\mathbf{R_0}$, that is known to lie within the region. This can, for example, be the location of the atom around which the elastic sheet has expanded. At each charge density point $\mathbf{R}_i$, a line is then drawn from the reference point through the charge density point,

$$\hat{\mathbf{r}}=\frac{\mathbf{R}_i-\mathbf{R_0}}{|\mathbf{R}_i-\mathbf{R_0}|}. \tag{16}$$

Of the particles defining the elastic sheet, the *M* particles closest to the line $\hat{\mathbf{r}}$ are found. We are currently using $M=20$. The location of these particles is projected onto a plane perpendicular to $\hat{\mathbf{r}}$. Then, using a method by D. F. Watson,[7] we triangulate in this plane the particles *M* to obtain the connectivity among particles. This connectivity is then used to reconstruct the surface of the ES locally as a collection of triangles in three-dimensional space. For each triangle, the equation

$$\alpha_1\mathbf{V}_1+\alpha_2\mathbf{V}_2+\alpha_3\mathbf{V}_3=\mathbf{R}_0+\lambda\hat{\mathbf{r}} \tag{17}$$

is solved. Here, the $\mathbf{V}_i$ are the coordinates of the vertices of the triangle being examined, λ measures the distance the triangle is from $\mathbf{R}_0$ along $\hat{\mathbf{r}}$, and α_i are the barycentric coordinates of the triangle. For a point to lie within the triangle,

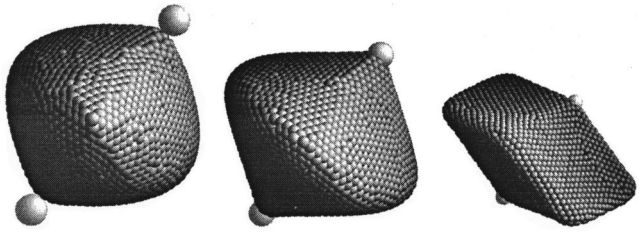

FIG. 2. Evolution of the elastic sheet around the valence electron density of a bond in a Si crystal. Starting with a perfect sphere, the first snapshot shown (left) is taken after 200 iterations, the second after 1000 iterations, and the third (right) after convergence to the zero-flux surface after 10 000 iterations. The larger spheres indicate the position of the Si atoms. The integrated charge of the enclosed volume is 1.976 electrons. The calculation took 34 min on a 400 MHz Pentium computer.

$\Sigma_i \alpha_i = 1$, so the constraint $\alpha_1 = 1 - \alpha_2 - \alpha_3$ is enforced. This gives a set of three linear equations with three unknowns. Solving this system for α_i, the line $\mathbf{R}_0 + \lambda \hat{\mathbf{r}}$ will cross the triangle defined by $\mathbf{V}_1$, $\mathbf{V}_2$, and $\mathbf{V}_3$ if and only if

$$0 \leqslant \alpha_i \leqslant 1, \ \forall i. \tag{18}$$

By solving this system of equations for each triangle in the triangulation, it can be determined which triangle the line crosses and at which point in space the line and the ES intersect,

$$\mathbf{R}_i' = \alpha_1 \mathbf{V}_1 + \alpha_2 \mathbf{V}_2 + \alpha_3 \mathbf{V}_3 . \tag{19}$$

The charge density point $\mathbf{R}_i$ is then inside the sheet if

$$|\mathbf{R}_i - \mathbf{R}_0| < |\mathbf{R}' - \mathbf{R}_0|. \tag{20}$$

For each point on the density grid, this method can be used to determine whether it is located in the region enclosed by the dividing surface.

This method will not work for complex surfaces where the line $\hat{\mathbf{r}}$ connecting a charge density point to the reference point can cross the elastic sheet more than once. More elaborate methods need to be used in such cases.

V. RESULTS

We have applied the above algorithm to partitioning of the valence electron densities obtained in DFT/PW91 pseudopotential[8] calculations of Si crystal, bulk ice, and water clusters containing from 2 to 6 water molecules. The Si structures studied include the bulk bond (Fig. 2), the bond between a pair of atoms which have been rotated in the Si crystal (Fig. 3), and the bond between the two atoms forming a dumbbell interstitial (Fig. 4). This last structure is especially complex, being composed of a total of five local maxima, leading to five different zero-flux surfaces to describe the valence charge density in the bonding region.

The bond in a perfect Si crystal (Fig. 2) should have an integrated charge density of 2 electrons. From the region enclosed by the converged elastic sheet using 2000 particles, which is shown in Fig. 2, the integrated charge density amounts to 1.977 electrons, within 1.1% of the expected value.

Figure 3 shows the zero-flux surface of the bond between two atoms that are rotated in the bulk. This configuration is metastable and is found along the minimum energy path of the concerted exchange process proposed by Pandey.[9] The integrated charge inside this surface is 2.097 electrons, showing that this bond has a slightly enhanced electronic density as compared with the perfect crystal.

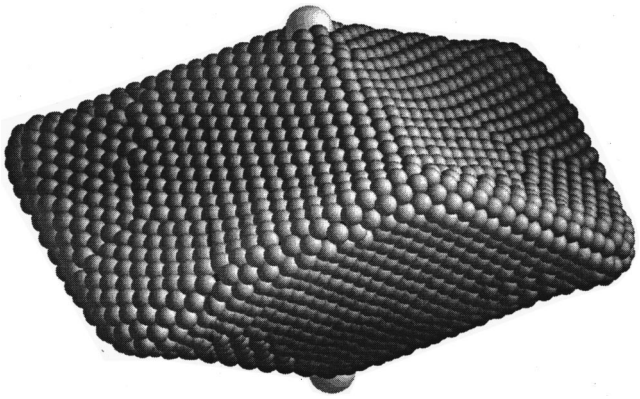

FIG. 3. Zero-flux surface for the bond between two atoms in the metastable state found along the minimum energy path of the concerted exchange Si diffusion process proposed by Pandey. The shape is very similar for the bond in the perfect crystal. The total integrated charge is larger for this bond, with the surface enclosing 2.097 electrons. The larger spheres show the location of the Si atoms.

A much more complicated topology of the zero-flux surface is associated with the split interstitial (also known as the dumbbell interstitial). The valence electron charge density for this bond is composed of five local maxima: a central maximum and four symmetric satellite maxima. Figure 4 shows the composition of these five surfaces. The total integrated charge density of the combined surfaces is 1.42 elec-

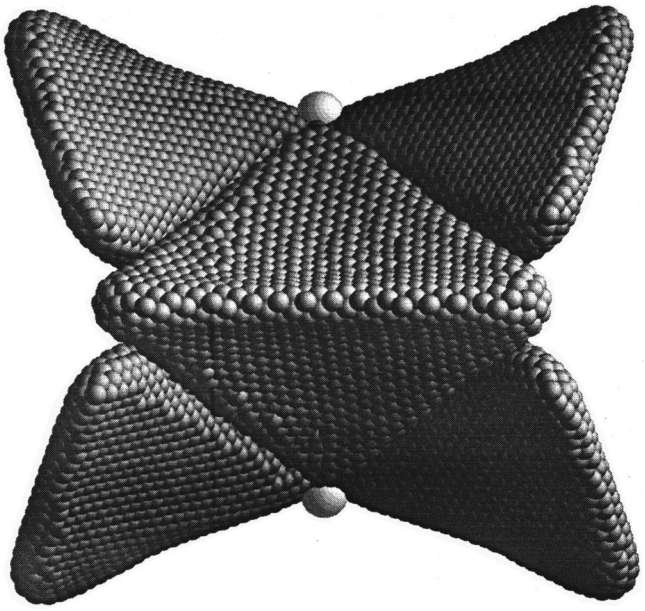

FIG. 4. Zero-flux surface for the bond between the two Si atoms forming a split interstitial configuration in a Si crystal. The valence charge density is decomposed into regions by zero-flux surfaces. The figure shows all five regions from the [100] Si crystal direction. The integrated charge of the central region is 0.86 electrons, while each of the satellite regions contains 0.14 electrons, giving a total of 1.42 electrons in the bond. The larger spheres indicate the location of the two Si atoms.

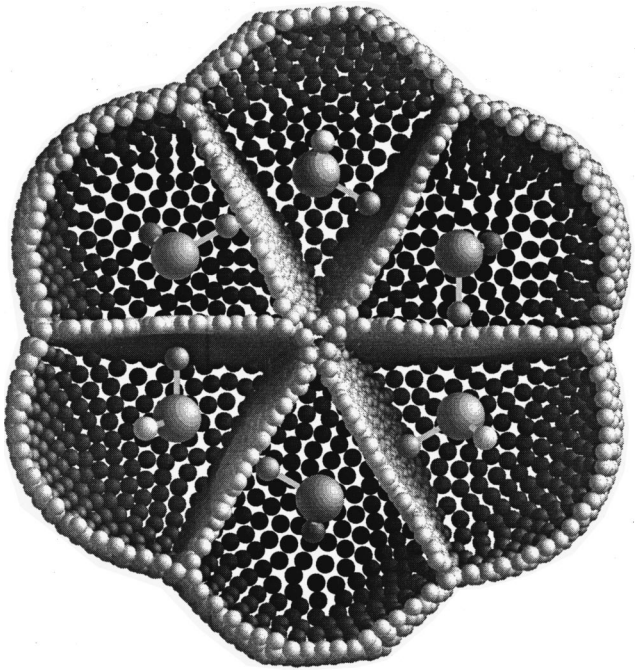

FIG. 5. Zero-flux surfaces for the six molecules in the water hexamer calculated from the valence charge density. Each of the surfaces was calculated separately. Of the total 48 valence electrons in the cluster, 47.96 are accounted for by the six subregions enclosed by the elastic sheets. The decomposition of the cluster charge density enabled calculation of the molecular multipole moments. The molecular dipole moment was found to be 2.47 D, up by 33% from the gas phase value. The outer boundary was chosen to be the $\rho=0.001$ electrons/Å^3 contour. The water molecules are also shown. Note the bending of the zero-flux surfaces near the hydrogen atoms.

trons, with 0.86 electrons in the central maximum and 0.14 electrons in each of the satellite maxima. These zero-flux surfaces are especially complex, with the central maximum exhibiting a very sharp cusp in the [100] direction and each of the satellite maxima containing two sharp points. As long as the smoothing force is included, the elastic sheet method describes these surfaces very well.

In a study of molecular multipole moments in water clusters, we used the elastic sheet method to identify Bader ''molecules'' in the clusters. The partitioning of the hexamer cluster is shown in Fig. 5. This figure illustrates how well the calculated subregions fill space. The six sheets were calculated separately. The final partitioning is cut so the inside is visible. There is some space in the very center of the partitioning that is not accounted for by the method (the size of the spheres hides that fact). However, most of the space of the system is accounted for by the subspaces. The total integrated valence density of the six H_2O molecules inside the calculated surfaces is 47.96 electrons, so the error is only 0.04 electrons out of 48.

The molecular multipole moments of the various H_2O molecules were calculated. Due to the effect of the electric field from neighboring molecules, the dipole moment increases from 1.86 D[10] in the gas phase to 2.47 D in the hexamer and 2.74 D in ice.[11] When the electric field was evaluated at a typical intermolecular distance from the cluster molecules, the multipole expansion using multipoles obtained from the Bader partitioning converged to the field obtained from the full electron density at the hexadecapole. We also compared calculations using the elastic sheet method with calculations based on the method of Stefanov and Cioslowski[3] using the GAUSSIAN94 code. While the calculation of the zero-flux surfaces for the hexamer did not converge, some of the other water clusters did converge, and the calculated molecular dipole moments then agreed to within 1% with our results from the elastic sheet method.

VI. DISCUSSION

During the development of the elastic sheet method, we have encountered several problems that had to be overcome. The biggest of these was the form of distributing force. As was mentioned before, we tune σ such that the nearest neighbors of a particle always lie on the repulsive side of the potential well. This repulsive pressure can in some cases force particles out of the sheet at sharp features such as points and cusps and into the neighboring zero-flux surfaces, forming winglike structures. One might think that a simple solution to this would be to choose an interaction resulting in attraction between nearest neighbors. When we tried this, however, holes formed in the sheet and the particles tended to clump together.

The addition of a ''smoothing'' force solved this problem. By adding a restoring force that tends to make the sheet locally flat, the particles are not allowed to escape from the dividing surface. Not only does this lead to smoother shape, but it also helps the long-term convergence. Without the smoothing force, the best estimate for the integrated charge of the bond in the Si crystal was 1.88 electrons. By adding the smoothing force, the integrated charge is 1.97 electrons, very close to the exact value of 2.00.

When the calculation is started, the particles are placed at random on a sphere centered on the atom of interest. The random placement of the particles will often cause very large forces between them, so the interaction force is scaled down in the first few steps of the minimization, until the particles have reached a reasonable distribution within the sphere.

VII. CONCLUSIONS

We have developed an elastic sheet method for finding the zero-flux dividing surfaces of the charge density. The method has been applied to a study of the electron density around interstitials in Si and in analysis of multipole moments of water molecules in water clusters. The discrete representation of the zero-flux surfaces obtained with the elastic sheet method can be used to calculate the integrated charge enclosed by the surface. The method should have more general applicability. The elastic sheet algorithm can be applied to any system where zero-flux surfaces of some scalar field are needed. It is possible to extend the method to higher dimensional systems, where it might, for example, be used to find the transition state dividing surface of a potential energy surface or even a free energy surface.

The computer program for carrying out elastic sheet calculations is available on request. The input for the calculation is simply the charge density evaluated on a uniform grid in three-dimensional space. An interpolation formula is then

used to evaluate the charge density at any point in space, as well as the gradient of the charge density.

ACKNOWLEDGMENTS

This work was supported by NSF Grant No. CHE-9710995. We gratefully acknowledge helpful discussions with Graeme Henkelman.

[1] R. S. Mulliken, J. Chem. Phys. **23**, 1833 (1955).
[2] R. F. W. Bader, *Atoms in Molecules—A Quantum Theory* (Oxford University Press, Oxford, 1990).
[3] B. B. Stefanov and J. Cioslowski, J. Comput. Chem. **16**, 1394 (1995).
[4] GAUSSIAN 98 User's Reference, p. 43, 2nd ed. (Gaussian Inc., 1999).
[5] G. Mills, H. Jónsson, and G. Schenter, Surf. Sci. **324**, 305 (1995); H. Jónsson, G. Mills, and K. W. Jacobsen, in *Classical and Quantum Dynamics in Condensed Phase Simulations*, edited by B. J. Berne, G. Ciccotti, and D. F. Coker (World Scientific, Singapore, 1998).
[6] H. C. Andersen, J. Chem. Phys. **72**, 2384 (1980).
[7] D. F. Watson, Comput. Geosci. **8**, 97 (1982).
[8] W. Kohn and L. J. Sham, Phys. Rev. **140**, A1133 (1965); M. C. Payne, M. P. Teter, D. C. Allen, T. A. Arias, and J. D. Joannopoulos, Rev. Mod. Phys. **64**, 1045 (1992); L. P. Perdew, *Electronic Structure of Solids '91* (Akademie Verlag, Berlin, 1991).
[9] K. C. Pandey, Phys. Rev. Lett. **57**, 2287 (1986).
[10] T. Dyke and J. Muenter, J. Chem. Phys. **59**, 3125 (1973).
[11] E. Batista, S. S. Xantheas, and H. Jónsson, J. Chem. Phys. **111**, 6011 (1999).